Proceedings of the 21st ICSMGE, Vienna, Austria, 14 – 19 June 2026. Pistrol, Adam & Schweiger (eds.)
Published by: ÖGG, Austrian Society for Geomechanics, Salzburg, Austria, ISBN 978-3-9503898-4-5
https://doi.org/10.53243/ICSMGE2026-1067

Numerical modelling of the Himalayan road-cut soil debris slope subjected to rainfall infiltration.

Samita Baniya, **Akanksha Tyagi**, Narendra Kumar Samadhiya
Civil Engineering Department, Indian Institute of Technology, Roorkee, Uttarakhand, India, akanksha.tyagi@ce.iitr.ac.in

ABSTRACT: Rainfall-induced landslides frequently threaten the Himalayan road infrastructure due to steep slopes, partially saturated soil, and intense monsoonal rainfall. This study models the effects of rainfall infiltration by talking into account of suction parameters to back-analyze the strength parameters of the Himalayan road-cut debris slope along National Highway 58 of Uttarakhand State, India. The soil and rocks were collected from the site, and were tested for geotechnical characterization in the laboratory. The seepage analysis was carried out in SEEP/W by applying rainfall on the slope surface as a flux boundary condition. The computed pore water pressures were then utilized as input in the SLOPE/W module of GeoStudio 2022 to evaluate the factor of safety using the limit equilibrium method. Results show a reduction in factor of safety during the peak monsoon due to matric suction loss, indicating critical instability when cohesion was reduced from 28.2 kPa to 10.35 kPa. The analysis showed that initially loss of matric suction leads to a sudden drop in FoS, while as the rainfall infiltration increases the FoS reduces due to the development of positive pore water pressures and induced seepage pressures.

KEYWORDS: Debris slopes, partially saturated slopes, numerical modelling, rainfall-induced instability

1 INTRODUCTION

As per the Geological Survey of India, the total area of 4.3 lakh sq. km, i.e., 13% of India's total geographical area, is prone to landslides. Among these landslide-prone areas, the Uttarakhand state is among the worst-hit states of India. Every monsoon season, many landslides occur, especially along National Highways in the Uttarakhand Himalayan slopes. Uttarakhand Himalaya forms an important part of the Himalayan range, with a mountainous topography. Uttarakhand is known as the home to several national parks, wildlife reserves, and several pilgrim areas, making it a heaven for biodiversity and tourism. Despite these merits, geological instability and hydro-meteorological variations are the major causes that have made this region one of the most disaster-prone states in the nation, emphasizing the need for sustainable development practices.

In the past, many researchers have studied the effect of rainfall infiltration on partially saturated slopes using numerical modelling. For example, Rahardjo et al. (2005); Raj and Sengupta (2014); Rahul et al. (2023) performed the uncoupled analysis, while Cai and Ugai (2004); Ering and Babu (2016); Pradhan et al. (2022); Rahul and Tyagi (2025) used coupled flow deformation analysis. However, such studies are scarce for Himalayan debris slopes.

The present study focuses on the numerical modelling of the Himalayan road-cut debris slope, considering suction parameters and rainfall infiltration. The geotechnical properties were obtained by performing laboratory tests on soil and rock samples. The soil water characteristics curve was obtained from the grain size distribution curve obtained by performing a sieve analysis test in the laboratory. The numerical modelling employed SEEP/W for transient seepage analysis and SLOPE/W for limit equilibrium analysis. The effect of rainfall was studied on the factor of safety (FoS) and pore water pressure distributions across the slope.

2 STUDY AREA

The study area is a 64 m high debris slope located along National Highway NH-58 (Rishikesh–Devprayag) near Gular, Uttarakhand. The geographical coordinates of the cutting are a Latitude of 30° 6'60.00" N and a Longitude of 78°26'0.00" E. The study area lies at an altitude of 1615 feet above the mean sea level. This debris slide lies on a sub-ridge slope, i.e., both on the uphill and downhill sides of the highway. The slope consists of bedrock overlain by debris overburden. The slope is composed of residual and colluvial deposits, which have experienced multiple events during each monsoon month. Road expansion activity along with the past rainfall events, has put the slope on the verge of failure since the year 2020 based on satellite images analyzed by Kundal and Bhardwaj (2025).

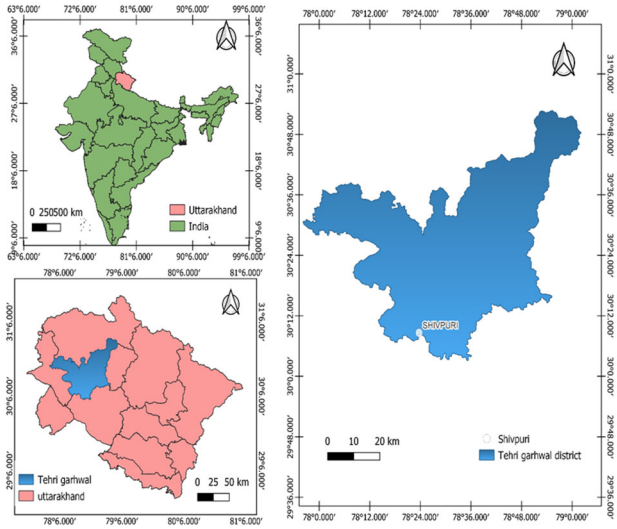

Figure 1. Location map of the study area from QGIS.

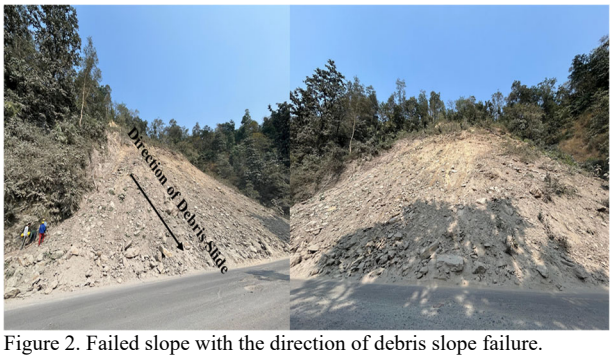

Figure 2. Failed slope with the direction of debris slope failure.

3 SOIL DEBRIS AND ROCK PROPERTIES

Soil debris and rock properties were evaluated at geotechnical laboratory, IIT Roorkee. The overburden soil debris material was classified as clayey gravel (GC) with a 22.67 % liquid limit and, 9.2 % plasticity index. The strength properties of soil

debris compacted at field unit weight (17.65 kN/m^3) and moisture content (5.4%), were evaluated from direct shear test using a shear box of size 300 mm x 300 mm x 20 mm. The cohesion c' and ϕ' were evaluated as 28.2 kPa and 34.9°, respectively. The coefficient of permeability of compacted specimen was obtained as approx. 4.32 × 10^{-5} m/s by falling head test. The axial test was performed on six rock samples having length to diameter ration of 0.3 to 1. The point load lump strength index test was performed on 10 samples. The uniaxial compressive strength (UCS) was then calculated using the empirical formulae relating the point load strength index and UCS. The average value of UCS from the axial test was found to be 65.44 kPa, and from the point load lump strength index test was found to be 63.24 kPa.

4 NUMERICAL MODEL AND INPUTS

4.1 *Geometry and Material Parameters*

Numerical modelling employed SEEP/W (for transient seepage) and SLOPE/W (for limit equilibrium analysis) in GeoStudio 2022. The slope has a base width of 122 meters with a slope height of 64 m and a bedrock depth of 10 meters below the ground surface (Figure 3). The mesh type used is quadrilateral and triangular, with the element size of 3 meters, with 821 nodes and 760 elements. The borehole data and geophysical investigation done on the slope using electrical resistivity tomography (ERT) survey showed the presence of overburden soil debris of up to 20 m or more. Thus, overburden soil debris material was assumed to be till road level, overlying bedrock. Tables 1 and 2 summarize the input properties for soil debris and bedrock for numerical modelling.

On the surface of the slope, rainfall intensity is applied as a flux boundary condition. The total head boundary condition is applied on the sides of the slope below the water table. The initial groundwater table is assumed to be at a 2 m from the bottom.

Table 1. Input parameters for soil debris material.

Properties	**Value**
Soil classification	Clayey Gravel (GC)
Material model	Mohr Coulomb
Unit weight (γ)	17.65 kN/m^3
Cohesion (c')	28.2 kPa
Frictional angle (ϕ′)	34.9 °
Saturated hydraulic conductivity (k_s)	1×10^{-5} m/s

Table 2. Input parameters for Bedrock.

Properties	**Value**
Material Model	Generalized Hoek-Brown criterion
Unit weight (γ)	20.48 kN/m^3
Unconfined compressive strength (UCS)	63240 kPa
Geological Strength Index (GSI)	20
Material constant (m_i)	11
Disturbance factor (D)	0

3.2. Volumetric Water Content and Hydraulic Conductivity Function

The volumetric water content function was developed from particle size information using the Modified Kovács model (for details, see Geo-Slope International Ltd., 2015). The grain-size-based method or the Modified Kovacs method (Aubertin et al. 2003) estimates the volumetric water content function using basic soil properties such as grain size distribution and liquid limit. The soil-water characteristics curve is shown in Figure 4.

The hydraulic conductivity function (Figure 5) was determined using (van Genuchten, 1980) model,

$$k_w = k_s \frac{[1-(a\Psi^{n-1})(1+(a\Psi^n)^{-m}]^2}{\left[\{(1+a\Psi)^n\}^{\frac{m}{2}}\right]} \quad (1)$$

Modified Mohr-Coulomb criterion was used for describing the shear strength of the unsaturated soil. From (Fredlund & Rahardjo 1993; Vanapalli et al. 1996),

$$s = c' + (\sigma_n - u_a)\tan\phi' + (u_a - u_w)\left[\left(\frac{\theta_w-\theta_r}{\theta_s-\theta_r}\right)\tan\phi'\right] \quad (2)$$

where s is the shear strength of the unsaturated soil, c' is the effective cohesion, $(\sigma_n - u_a)$ is the net normal stress, $(u_a - u_w)$ is the matric suction, ϕ' is the effective angle of internal friction, θ_w is the volumetric water content, θ_r is the residual volumetric water content, and θ_s is the saturated volumetric water content.

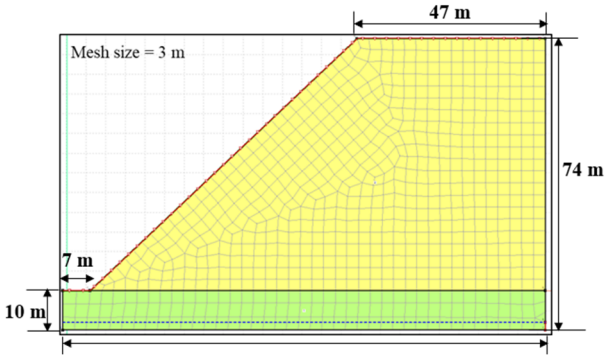

Figure 3. Geometry of the Slope Showing Mesh and Position of the Water Table.

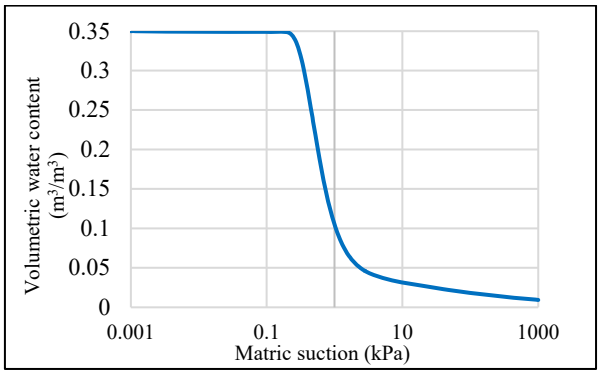

Figure 4. Soil-Water Characteristic Curve.

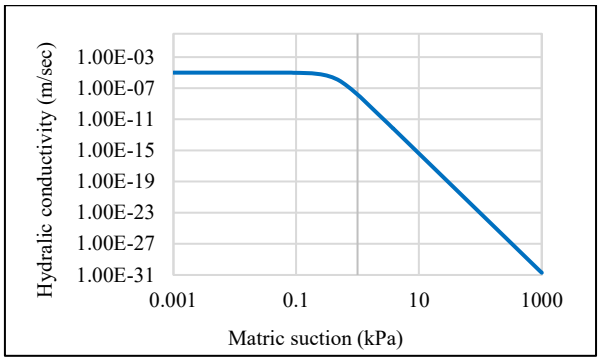

Figure 5. Hydraulic Conductivity Function Curve.

3.3. Rainfall Data

The rainfall data for the year 2020 was obtained from the Indian Meteorological Department (IMD) website for the 0.25 × 0.25 gridded data and are plotted in Figure 5.3. A total of 2915.85 mm of rainfall was observed in the year 2020, out of which 108.97 mm was observed as the maximum rainfall on the 2nd of August. Similarly, July has the maximum cumulative rainfall, which was equal to 811.56. This rainfall data was used as input for infiltration in the analysis.

3.4. Factor of Safety Determination

Uncoupled analysis was adopted herein in Geostudio 2022. In the UFD analysis, mechanical deformation and fluid flow are computed separately. SEEP/W is used for conducting seepage analysis, and SLOPE/W is used for conducting slope stability analysis. The first step involves performing a seepage analysis in SEEP/W to calculate the pore water pressure (PWP) in a slope over a specific period. The computed PWP are then utilized to calculate deformations in SLOPE/W, followed by the slope stability assessment using the limit equilibrium method. Morgenstern and Price (1965) method was used to determine the factor of safety (FoS).

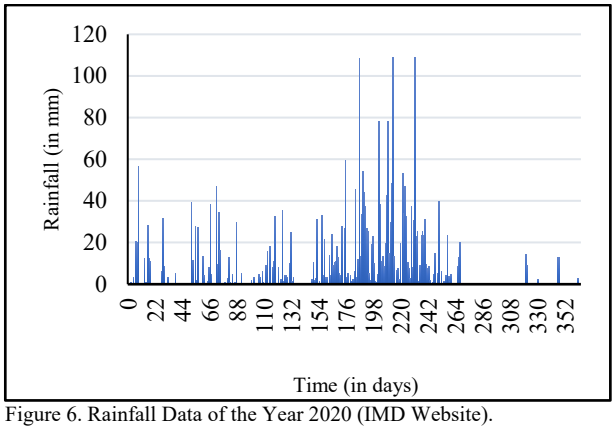

Figure 6. Rainfall Data of the Year 2020 (IMD Website).

5 RESULTS AND DISCUSSION

5.1. Variation of FoS with Time

For the analysis, initial effective cohesion c’ and effective friction angle ϕ’ of 28.2 kPa and 34.9° were adopted.

As shown in Figure 7, the FoS drops with the rainfall infiltration. The sudden initial drop in FoS corresponds to the early stage of rainfall infiltration. Initially, due to the unsaturated condition of the clayey gravel at this stage, matric suction had provided additional shear strength to the slope.

However, as rainfall continues to infiltrate, the suction starts reducing gradually, which leads to a decrease in FoS. After the sudden drop, FoS remains relatively stable (1.2058) for an extended period, i.e., 10 to 225 days, because of the maintenance of matric suction and limited saturation in the unsaturated zone.

Afterward, there is a significant reduction in FoS between 225-240 days, as they coincide with the peak rainfall period (July cumulative 811.56 mm, August daily peak 108.97 mm). This decline in FoS to 1.2054 is due reduction in suction and also a loss of effective stress due to rising pore pressures because of infiltration. In the subsequent period (240-350 days), the FoS shows a gradual decline (to 1.2052) due to cumulative saturation effects. For the adopted c’ and ϕ’, the slope did not show any failure, i.e., the FoS did not fall to unity.

5.2. Back-Analysis using UFD analysis

For the given soil debris material, the value of the plasticity index was 9.2. Hence, the input value of ϕ’ was well within the range of 30° to 40° suggested by Duncan (1992). Therefore, the value of ϕ’ was kept constant, while the value of c’ was progressively reduced until the FOS reached 1 or slightly below.

Figure 8 shows that for a c’ of 10.35 kPa, the initial FoS was approximately 1.0015 under dry conditions. From Day 0 to Day 3.64, the FoS is slightly decreasing. This stage shows the beginning of rainfall infiltration and matric suction contributing to the stability of the slope. The PWP distribution for a day is further shown in Figure 9. As rainfall infiltrates the upper soil layers, matric suction starts to reduce in near-surface zones. This reduction leads to a minor reduction in shear strength and thus FoS. The groundwater table position remains almost at its initial level during this period.

Between Day 3.64 to Day 7.28, there is a sharp drop in FoS. This represents a critical transition point in slope stability resulting from a significant rise in PWP during this period as the rainfall infiltration reached deeper layers. Between day 7.28 to day 230, the FoS seems to be constant. This period shows a continuous increase in pore water pressure and continued saturation. The continued rainfall infiltration prevented the recovery of the matric suction. The GWT position continued to rise in lower zones of the slope, leading to a gradual weakening of soil strength over time. As a result, the slope stayed weakened without further major changes in FoS. From Day 230 to Day 244, the FoS showed a slight drop. This is due to localized rainfall infiltration causing a rapid increase in PWP in some slope regions and slightly lowering FoS.

Between Day 244 and Day 346 (dry period), the FoS trend appears to be stable, suggesting that the slope has reached a near steady-state saturation condition. As the rainfall infiltration progressed, pore water pressure increased and suction decreased, reducing effective stress. Hence for this reduced cohesion value of 10.35 kPa, the FOS drops below unity at the 344th day (Figures 8 and 10). However, it should be noted that the cut-slope was on the verge of failure with FoS close to unity, even without rainfall for this cohesion value.

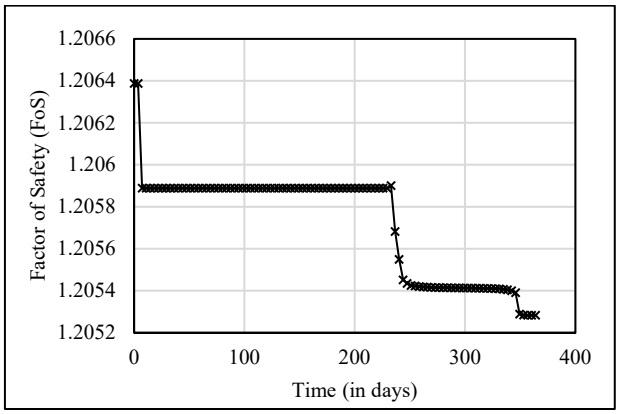

Figure 7. FoS vs Time for c' = 28.2 kPa and ϕ' = 34.9°.

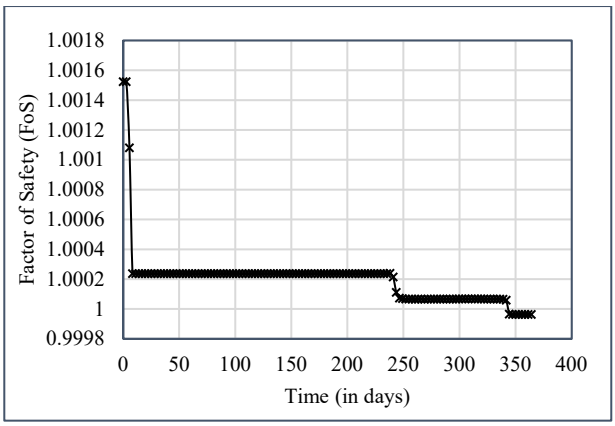

Figure 8. FoS vs Time for c' = 10.35 kPa and ϕ' = 34.9°.

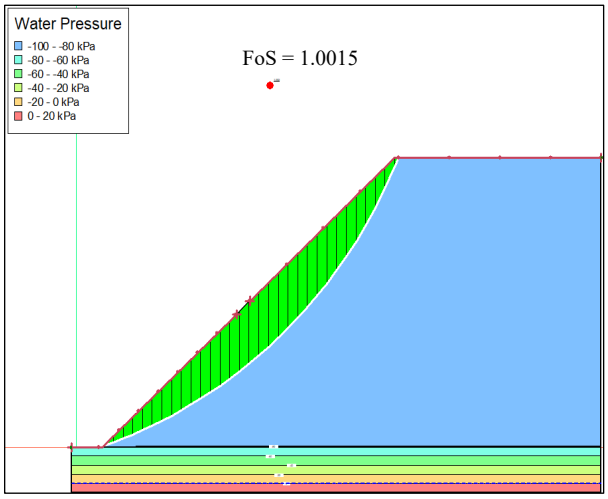

Figure 9. Critical slip circle and pore water pressure distribution under dry conditions (Day 0), for c' = 10.35 kPa and ϕ' = 34.9°.

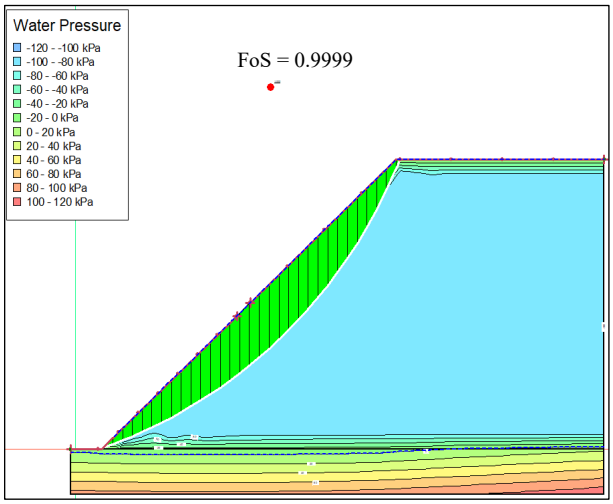

Figure 10. Critical slip circle and pore water pressure distribution under dry conditions (Day 364), for c' = 10.35 kPa and ϕ' = 34.9°.

6 CONCLUSION

The paper discusses an investigation on the stability analysis of road-cut debris slope along National Highway NH-58 of Uttarakhand Himalaya, India. This study integrates field survey, laboratory testing, and numerical modelling. Following are the major findings from the study:

- The laboratory testing shows that the soil was of low plasticity, with c' = 28.2 kPa and ϕ' = 34.9°. Similarly, bedrock was found to have a unit weight of 20.48 kN/m^3 and uniaxial compressive strength of 63.240 MPa.
- The volumetric water content function was developed from particle size information using the Modified Kovács model.
- The numerical analysis showed the influence of rainfall infiltration on slope stability. The analysis found that initially, loss of matric suction led to a sudden drop in FoS, while as the rainfall infiltration increased, the FoS reduced due to the development of positive pore water pressures and induced seepage pressures as a result of rainfall infiltration.
- The deterministic back analysis using UFD was conducted, and c' =10.35 kPa was obtained, corresponding to FoS dropping below unity at 340 days of rainfall. However, it should be noted that the cut-slope was on the verge of failure with FoS close to unity, even without rainfall for this cohesion value.

6 ACKNOWLEDGEMENT

This study was supported by the Ministry of Road Transport and Highways (MoRTH), Government of India, under the sponsored research project MRT-2270-CED/23-24. The authors would like to acknowledge the assistance of Suraj Kumar, Junior Research Fellow, IIT Roorkee during soil collection and laboratory testing.

7 REFERENCES

Rahardjo, H., Lee, T.T., Leong, E.C. and Bezaur. 2005. Response of a residual soil slope to rainfall. *Canadian Geotechnical Journal*, 42, 340-351.

Raj, M. and Sengupta, A. 2014 Rain-triggered slope failure of the railway embankment at Malda, India. *Acta Geotechnical* 9(5), 789–798.

S. Rahul, P. Shadani, A. Tyagi 2023 Stability of Lateritic Soil Cutting of Maharashtra Subjected to Rainfall Infiltration. *Indian Geotech. Conference 2023,* Roorkee, India.

Cai, F. and Ugai, K. 2004 Numerical Analysis of Rainfall Effects on Slope Stability. *Int. J. Geomech* 4, 69-78.

Ering, P. and Babu, G.L.S. 2016 Probabilistic back analysis of rainfall induced landslide- A case study of Malin landslide, India. *Engineering Geology* 208, 154–164.

Pradhan, S., Toll, D.G.., Rosser, N.J., Brain, M.J. 2022. An investigation of the combined effect of rainfall and road cut on landsliding. *Engineering Geology*, 307, 106787.

Rahul, S. and Tyagi, A. 2025 Physics based time of failure determination of rainfall induced instability in lateritic soil slopes. *Engineering Geology* 344, 107834.

Kundal, S., Bhardwaj, A. 2025. Personal Communication, Indian Institute of Technology Roorkee.

GEO-SLOPE International Ltd. 2015. Seepage Modeling with SEEP/W, GeoStudio. Calgary, Alberta, Canada.

Aubertin, M., Mbonimpa, M., Bussière, B. and Chapuis, R.P. 2003. A model to predict the water retention curve from basic geotechnical properties. *Canadian Geotechnical Journal*, 40(6), 1104- 1122.

Van Genuchten, M.T. 1980 A Closed-form Equation for Predicting the Hydraulic Conductivity of Unsaturated Soils. *Soil Science Society of America Journal* 44(5), 892–898.

Fredlund, D.G. and Rahardjo, H. 2002. *Soil Mechanics for Unsaturated Soils*, *Soil Mechanics for Unsaturated Soils*. *John Wiley and Sons Inc.*

Vanapalli, S.K., Fredlund, D.G., Pufahl, D.E., Clifton, A.W. 1996. Model for the prediction of shear strength with respect to soil suction. *Canadian Geotechnical Journal*, 33(3), 379–392.

Morgenstern, N.R. and Price, V.E. 1965 The Analysis of the Stability of General Slip Surfaces. *Géotechnique* 15(1), 79–93.

Duncan, J.M. 1992 Soil strengths from back-analysis of slope failures *Proc. of Specialty Conf. Stability and Performance of Slopes and Embankments-II* 1, pp. 890–904.